Study of the CO_2 Transfer Rate in a Reacting Flow for the Refined Sodium Bicarbonate Production Process

Christophe Wylock[*1], Aurélie Larcy[1], Pierre Colinet[1], Thierry Cartage[2] and Benoît Haut[1]
[1]Université Libre de Bruxelles, [2]Solvay S.A.
*Corresponding author: Av. FD Roosevelt 50, CP 165/67, 1050 Brussels, cwylock@ulb.ac.be

Abstract: This work deals with the quantification of the CO_2 transfer rate from a bubble to the surrounding liquid in a bubble column. A model is successfully developed using COMSOL Multiphysics. The validated model is used to study the enhancement influence of chemical reactions on the transfer rate. More, the results of this study are compared with a classical 1-D approach and an excellent comparison is observed.

Keywords: chemical engineering, gas-liquid mass transfer, bubble columns

1. Introduction

The sodium bicarbonate production process is one of the oldest processes of the Solvay group. The main step of the production process is the dispersion, under the form of bubbles, of a gaseous mixture of air and CO_2 in a brine (aqueous solution rich in Na^+ and $CO_3^=$). This dispersion is realized in large bubble columns, called the BIR columns.

This work deals with the quantification of the CO_2 transfer rate from a bubble, rising in the liquid phase, to the brine. The main resistance to this transfer is located in the liquid phase. In this phase, the convective transport of CO_2 by the liquid flow is coupled with its diffusive transport and with chemical reactions. Therefore, it is necessary to take these three phenomena into account simultaneously to quantify the CO_2 transfer rate.

The presence of adsorbed surfactants at the interface of the bubble has a strong influence on the mass transfer as it can change the flow field around the bubble [1]. Therefore, two cases are investigated: a fully contaminated bubble and a clean bubble.

2. 2-D Modelling and Simulation

2.1 Governing equations

A pure CO_2 spherical bubble, moving upward at a steady velocity in a liquid at rest and of infinite extent, is considered. In the liquid phase, the transferred CO_2 takes part to the two following chemical reactions [2,3,4] :

$$CO_2 + OH^- \rightleftharpoons HCO_3^- \qquad (1)$$

$$HCO_3^- + OH^- \rightleftharpoons CO_3^= + H_2O \qquad (2)$$
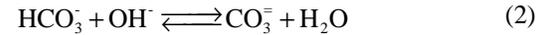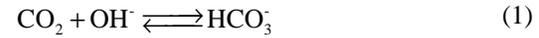
The balance equations are written in dimensionless form in an inertial reference frame located at the mass center of the bubble.

The bubble velocity G, the bubble diameter d_b, and ρG^2, where ρ is the liquid density, are used as reference velocity, length and pressure, respectively. The interfacial CO_2 concentration $[CO_2]_i$ and the OH^-, HCO_3^- and $CO_3^=$ bulk concentrations, $[OH^-]_{bulk}$, $[HCO_3^-]_{bulk}$ and $[CO_3^=]_{bulk}$, are used as reference concentrations.

Let $\boldsymbol{u}$ be the dimensionless liquid velocity vector, p the dimensionless pressure and a, b, c, and d the dimensionless concentrations of the CO_2, OH^-, HCO_3^- and $CO_3^=$, respectively.

At steady state, the vectorial form of the incompressible Navier-Stokes and continuity equations coupled with the convection-diffusion-reaction equations, write as follows [5,6]:

$$\begin{cases} (\boldsymbol{u}\boldsymbol{\cdot}\boldsymbol{\nabla})\boldsymbol{u} = \boldsymbol{\nabla}\boldsymbol{\cdot}\left[-p\mathbf{I}+\frac{1}{Re}\left(\boldsymbol{\nabla}\boldsymbol{u}+\left(\boldsymbol{\nabla}\boldsymbol{u}\right)^{\mathrm{T}}\right)\right] \\ \boldsymbol{\nabla}\boldsymbol{\cdot}\boldsymbol{u} = 0 \end{cases} \qquad (3)$$

$$\begin{cases} \boldsymbol{\nabla}\boldsymbol{\cdot}\left(-\frac{1}{Pe}\boldsymbol{\nabla}a\right)=-r_1 -(\boldsymbol{u}\boldsymbol{\cdot}\boldsymbol{\nabla})a \\ \boldsymbol{\nabla}\boldsymbol{\cdot}\left(-\frac{\beta_b}{Pe}\boldsymbol{\nabla}b\right)=\chi_b\left(-r_1 -r_2\right)-(\boldsymbol{u}\boldsymbol{\cdot}\boldsymbol{\nabla})b \\ \boldsymbol{\nabla}\boldsymbol{\cdot}\left(-\frac{\beta_c}{Pe}\boldsymbol{\nabla}c\right)=\chi_c\left(r_1 -r_2\right)-(\boldsymbol{u}\boldsymbol{\cdot}\boldsymbol{\nabla})c \\ \boldsymbol{\nabla}\boldsymbol{\cdot}\left(-\frac{\beta_d}{Pe}\boldsymbol{\nabla}d\right)=\chi_d r_2 -(\boldsymbol{u}\boldsymbol{\cdot}\boldsymbol{\nabla})d \end{cases} \qquad (4)$$

Re is the classical particle Reynolds number, defined as:

$$Re = \frac{Gd_b}{\upsilon} \qquad (5)$$

where υ is the liquid kinematic viscosity.

Pe is the Peclet number, which can be calculated by $Pe=Re.Sc$, where Sc is the Schmid number, defined as:

$$Sc = \frac{v}{D_{CO_2}} \qquad (6)$$

where D_{CO_2} is the CO$_2$ diffusion coefficient.

r_1 and r_2 are the chemical reaction rates. They are written:

$$r_1 = Ha_1^2\left(ab - \alpha c\right) \qquad (7)$$

$$r_2 = Ha_2^2\left(bc - d\right) \qquad (8)$$

where $\alpha=[CO_2]_{bulk}/[CO_2]_i$ is the CO$_2$ concentration ratio between the bulk and the interface and Ha_1 and Ha_2 are the Hatta numbers for the reactions (1) and (2), defined as:

$$Ha_1 = \sqrt{k_{11}[OH^-]_{bulk}\frac{d_b}{G}} \qquad (9)$$

$$Ha_2 = \sqrt{k_{21}\frac{[OH^-]_{bulk}[HCO_3^-]_{bulk}}{[CO_2]_i}\frac{d_b}{G}} \qquad (10)$$

where k_{11} and k_{21} are the kinetic constants of the reactions (1) and (2), respectively.

$\beta_b = D_{OH^-}/D_{CO_2}$, $\beta_c = D_{HCO_3^-}/D_{CO_2}$ and $\beta_d = D_{CO_3^=}/D_{CO_2}$ are the ratios of diffusion coefficients and $\chi_b = [CO_2]_i/[OH^-]_{bulk}$, $\chi_c = [CO_2]_i/[HCO_3^-]_{bulk}$ and $\chi_d = [CO_2]_i/[CO_3^=]_{bulk}$ are the ratios of bulk concentrations.

This work is limited to an axisymmetrical flow. In the case of a clean bubble, no vortex appears and the wake remains steady and axi-symmetric if $Re<500$. For a fully contaminated bubble behaving as a solid sphere, the wake presents a steady axi-symmetric vortex for $Re>20$ and loses its axi-symmetry at $Re=210$ [1,5].

2.2 Flow domain and boundary conditions

The axisymmetrical computational domain is presented in Figure 1. A semi bubble is located at the center of a semi circular domain. The domain diameter in dimensionless form is 10.

The inlet is located at the top boundary of the flow domain, where uniform downward velocity and initial concentrations are imposed:

$$u = 0 \text{ , } v = -1 \qquad (11)$$

$$a = \alpha \text{ , } b = 1 \text{ , } c = 1 \text{ , } d = 1 \qquad (12)$$
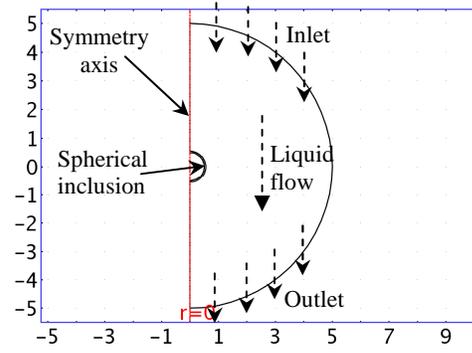
Figure 1. Diagram of the geometry.

At the bottom of the domain, a stress-free condition is imposed and the flux of the different species is purely convective:

$$\left[-p\mathbf{I} + \frac{1}{Re}\left(\nabla\boldsymbol{u} + \left(\nabla\boldsymbol{u}\right)^{\mathrm{T}}\right)\right]\mathbf{n} = 0 \qquad (13)$$

$$\mathbf{n}\cdot\left(-\frac{\nabla a}{Pe}\right) = 0 \text{ , } \mathbf{n}\cdot\left(-\frac{\beta_b\nabla b}{Pe}\right) = 0,$$

$$\mathbf{n}\cdot\left(-\frac{\beta_c\nabla c}{Pe}\right) = 0 \text{ , } \mathbf{n}\cdot\left(-\frac{\beta_d\nabla d}{Pe}\right) = 0 \qquad (14)$$

where $\mathbf{n}$ is the normal vector.

On the bubble surface, only the a specie is able to diffuse through the interface and its concentration is assumed to be uniform. Therefore, the boundary conditions write as follows :

$$a = 1 \text{ , } \mathbf{n}\cdot\left(-\frac{\beta_b\nabla b}{Pe} + b\boldsymbol{u}\right) = 0 \text{ , } \qquad (15)$$

$$\mathbf{n}\cdot\left(-\frac{\beta_c\nabla c}{Pe} + c\boldsymbol{u}\right) = 0 \text{ , } \mathbf{n}\cdot\left(-\frac{\beta_d\nabla d}{Pe} + d\boldsymbol{u}\right) = 0$$

In the case of a fully contaminated bubble, the bubble behaves as a solid sphere [1,5]. Therefore, a no slip condition is imposed at the surface of the bubble:

$$\boldsymbol{u} = 0 \qquad (16)$$

For a clean bubble, a slip condition is imposed, therefore the normal component of the velocity and the shear stress are equal to zero at the surface of the bubble:

$$\mathbf{n}\cdot\boldsymbol{u} = 0 \text{ , } \mathbf{t}\cdot\left(-p\mathbf{I} + \frac{1}{Re}\left(\nabla\boldsymbol{u} + \left(\nabla\boldsymbol{u}\right)^{\mathrm{T}}\right)\right)\mathbf{n} = 0 \qquad (17)$$

2.3 Use of COMSOL Multiphysics

The Incompressible Navier-Stokes mode coupled with Convection and Diffusion mode, from the Chemical Engineering Module, are used

in 2-D axisymetric geometry. All the simulations are performed with the version 3.3.0.405 of COMSOL Multiphysics.

2.4 Meshing

To mesh the domain, a concentric circular mapped mesh is used (23140 elements). It has been observed that a mapped mesh gives a far better convergence and better results for the convection-diffusion equations than a free mesh, especially in the drag zone at the rear of the bubble.

As it is presented in Figure 2, a finer mesh is used in the vicinity of the interface. The dimensionless thickness of this dense mesh zone is 0.05 and the thickness of the first mesh close to the bubble is $8.3 \ 10^{-4}$.

It can be demonstrated that the diffusion boundary layer normalized by the bubble diameter can be roughly estimated by $1/\sqrt{Pe}$ [7]. In this work, the smallest value of Pe is 5000. Therefore, it is ensured that the diffusion boundary layer does not lie beyond this zone.

To create the mesh, a chosen number of node points are imposed on the bubble surface (392 points) and on the symmetry axis (30 points in the dense mesh zone and 80 points outside, above and below the bubble).

2.5 Simulation procedure

Assuming that the mass transfer and the resulting chemical reactions do not influence the liquid flow, momentum transport and mass transport are solved separately.

The Navier-Stokes equations are solved first without mass transfer. The initial condition is no flow:
$$u = 0 , v = 0 \tag{18}$$
The resulting computed flow is then stored.

In a second step, the diffusion-convection problem is solved without chemical reactions using the flow field calculated at the previous step. The initial concentration fields are:
$$a = \alpha , b = 1 , c = 1 , d = 1 \tag{19}$$
The resulting concentration fields are stored to be used as new initial conditions.

Finally, the convection-diffusion-reaction problem is solved, using the flow field from the first step and the concentration fields form the second step.
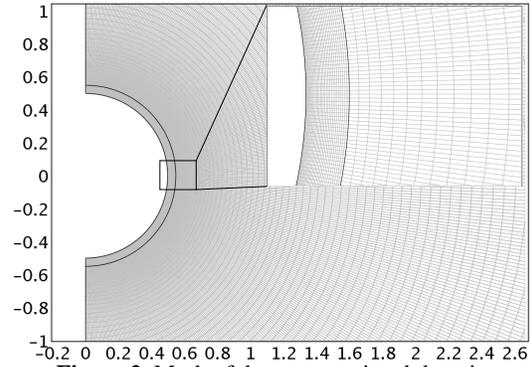
Figure 2. Mesh of the computational domain.

For each step, the stationary direct solver UMFPACK is used.

3. Validation Without Reaction

In order to validate the modeling with COMSOL Multiphysics, the numerical simulation results are first compared with literature correlations concerning the drag coefficient C_D and the Sherwood number Sh for both clean and fully contaminated bubbles.

Considering the boundary values of the Reynolds number for the validity of an axisymmetrical flow simulation, the validation for the clean bubble is therefore realized for $20 \leq Re \leq 400$ and for the fully contaminated bubble for $10 \leq Re \leq 200$.

The drag coefficient is the dimensionless form of the average of the z-components of the shear stress and the non-hydrostatic component of the pressure on the bubble surface, defined as:
$$C_D = \frac{8}{\pi} \oint (-p_z + (-\tau_{rz} + \tau_{zz})) \ dS \tag{20}$$
where p_z is the z-component of the pressure and τ_{rz} and τ_{zz} are the z-components of the shear stress.

The average Sherwood number is the dimensionless mean mass transfer rate from the bubble to the liquid. It is calculated from the dimensionless a flux integration along the bubble surface, as follows:
$$Sh = -\frac{1}{\pi(1-\alpha)} \oint \nabla a \ dS \tag{21}$$

For a solid sphere, a recirculatory wake is formed at the rear of the bubble when $Re > 20$ [1,5]. Therefore, the separation angle is also compared with the literature for the fully contaminated bubble.

3.1 Drag coefficients

The comparison of the COMSOL drag coefficient and the literature correlations is presented as a function of the Reynolds number in Figure 3.

In the case of the clean bubble, the COMSOL results are compared with correlations from:
- Hamielec *et al.* (for 4<*Re*<100) [1]:

$$C_D = 13.725 \ Re^{-0.74} \tag{22}$$

- Hass *et al.* (for *Re*>2) [1]:

$$C_D = 14.9 \ Re^{-0.78} \tag{23}$$

For the fully contaminated bubble behaving as a solid sphere, the numerical results are compared with correlations from:
- Lapple *et al.* (for *Re*<1000) [1] :

$$C_D = \frac{24}{Re}\left(1 + 0.125 \ Re^{0.172}\right) \tag{24}$$

- Clift *et al.* [1]:

$$0.01 < Re \le 20 \rightarrow C_D = \frac{24}{Re}\left(1 + 0.1315 Re^{0.82 - 0.05\log_{10} Re}\right) \tag{25}$$

$$20 < Re \le 260 \rightarrow C_D = \frac{24}{Re}\left(1 + 0.1935 Re^{0.6305}\right)$$

It is observed that the drag coefficients computed by the COMSOL model are in excellent agreement with these correlations.

3.2 Separation angle for a solid sphere

For the fully contaminated bubble, the separation angle calculated by the model is compared with the correlation proposed by Clift *et al.* (for 20<*Re*<400) [1] :

$$\theta_s = 180 - 42.5 \ \left(\log\left(Re/20\right)\right)^{0.483} \tag{26}$$

The results, which are presented in Figure 4, show an excellent agreement.

3.3 Sherwood number

The comparison of the COMSOL Sherwood number and the literature correlations for *Sc*=500 is presented in Figure 5 as a function of the Reynolds number.

For the clean bubble, the simulation results are compared with correlations from:
- Lochiel and Calderbank (for $Re \gg 1$) [5]:

$$Sh = \frac{2}{\sqrt{\pi}}\left(1 - \frac{2.96}{Re^{0.5}}\right)^{0.5} Pe^{0.5} \tag{27}$$
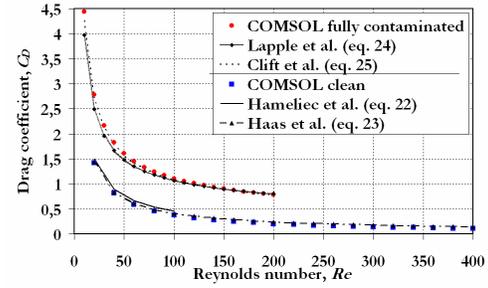
Figure 3. Drag coefficient versus Reynolds number for clean bubble and fully contaminated rigid bubble.
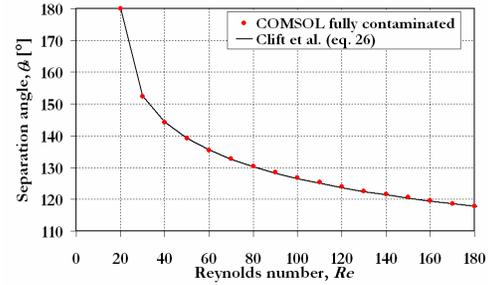
Figure 4. Separation angle versus Reynolds number for fully contaminated rigid bubble.
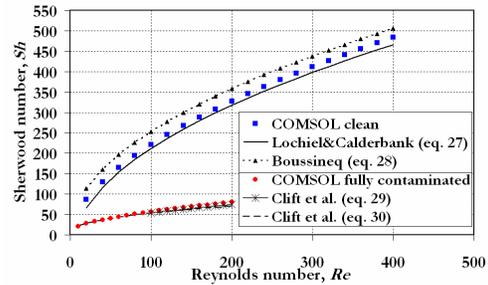
Figure 5. Sherwood number versus Reynolds number for clean bubble and fully contaminated rigid bubble.

- Boussineq (for $Re \gg 1$) [1]:

$$Sh = 1 + \frac{2}{\sqrt{\pi}} Pe^{0.5} \tag{28}$$

For the fully contaminated bubble, the two following correlations, proposed by Clift *et al.*[1], are used:

$$Sh = 1 + 0.724 \ Re^{0.48} Sc^{1/3} \tag{29}$$

(for 100<*Re*≤2000 and *Sc*>200)

$$Sh = 1 + \left(1 + \left(1/\left(Re \ Sc\right)\right)^{1/3} Re^{0.41}\right) Sc^{1/3} \tag{30}$$

(for 1≤*Re*≤400 and 0.25≤*Sc*≤100)

For both cases, a good agreement is observed.

3.4 Preliminary conclusion

The results of this validation step show the ability of the COMSOL simulations to estimate, with a good agreement, the hydrodynamic and the gas-liquid mass transfer parameters for different bubble cases for which well known data can be found in the literature. The model is then considered validated.

4. Simulation Results and Discussion

In this section, the effect of the chemical reaction kinetics on the mass transfer rate is studied by varying the values of Ha_1 and Ha_2, for the operating conditions in a BIR column.

The bubbles have an average diameter of 1 mm and a rising velocity of 0.2 m/s. Therefore, the simulations are realized with Re=200 and Sc=500. Other parameters have been calculated using correlations from Vas Bhat $et\ al.$ [3]. Their values are : $\alpha = 0.003$, $\chi_b = 64$, $\chi_c = 0.03$, $\chi_d = 0.025$, $\beta_b = 4.1$, $\beta_c = 0.9$, $\beta_d = 0.7$, $Ha_1 = 0.19$, $Ha_2 = 902$.

Since Ha_2 is much greater than Ha_1, the mass transfer is not very sensitive to the Ha_2 value. It has been confirmed by a sensitivity analysis. Therefore, the Sherwood number is computed for different values of Ha_1.

The a-concentration fields for different Ha_1 values and for both clean and fully contaminated bubbles are presented in Figure 6.

As expected, it is observed that the chemical reactions deplete the concentration of the transferred specie in the liquid phase for increasing Ha_1 number. At Ha_1=10, the a-specie is totally consumed beyond the diffusion boundary layer. Furthermore, it is observed that the size of this diffusion boundary layer decreases when Ha_1 increases.

In order to quantify the effect of the chemical reaction rates on the transfer rate, the Sherwood number Sh and the chemical enhancement factor E are calculated.

The enhancement factor, E, is defined as the ratio [8] of the transfer rate when reactions are coupled with diffusion on the transfer rate in purely diffusive regime. It is calculated by dividing the Sherwood number with reactions by the Sherwood number without reaction. The Sherwood number and the enhancement factor results are presented in Figure 7.
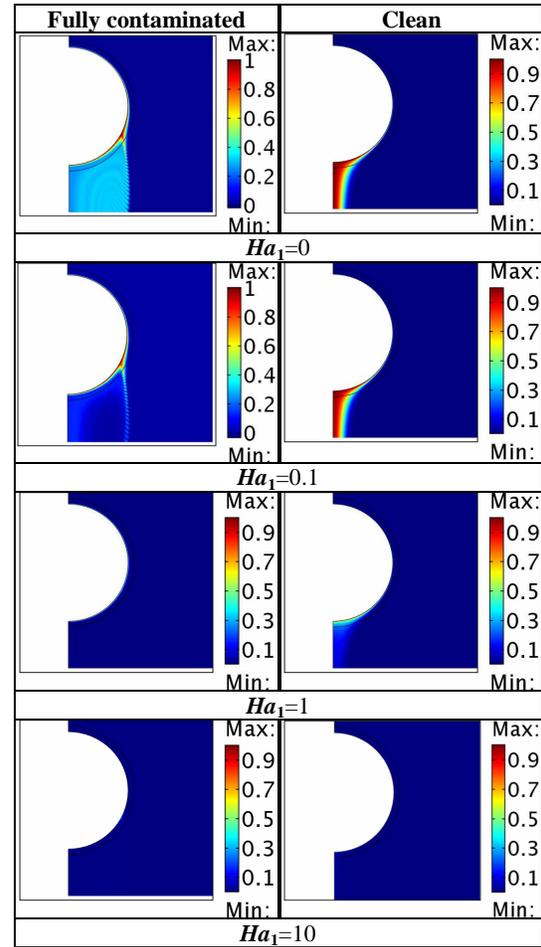
Figure 6. Surface concentration fields of a specie for both fully contaminated (left) and clean (right) bubbles for several values of Ha_1.

It is observed that the chemical reactions increase the CO_2 transfer rate, especially when the Ha_1 number is higher than 1. The effect of the chemical reactions is more important in the fully contaminated bubble case, but the Sherwood number remains larger in the case of the clean bubble.

A commonly-used approach to estimate the gas-liquid transfer rate in a chemical reactor is the uni-dimensional Higbie model [9].

In this approach, the liquid flow is idealized as a mosaïc of liquid elements slipping around the bubble. Each element stays in contact with the bubble the same time, there is no shear stress in the liquid and the diffusion is normal to the interface. Therefore, the evolution of the concentrations in these elements is modeled by a

1-D equation system. The dimensionless form of the mass transport equations writes as:

$$\begin{cases} \dfrac{\partial a}{\partial t} = \dfrac{1}{Pe}\dfrac{\partial^2 a}{\partial x^2} - r_1 \\[2mm] \dfrac{\partial b}{\partial t} = \dfrac{\beta_b}{Pe}\dfrac{\partial^2 b}{\partial x^2} + \chi_b\left(-r_1 - r_2\right) \\[2mm] \dfrac{\partial c}{\partial t} = \dfrac{\beta_c}{Pe}\dfrac{\partial^2 c}{\partial x^2} + \chi_c\left(r_1 - r_2\right) \\[2mm] \dfrac{\partial d}{\partial t} = \dfrac{\beta_d}{Pe}\dfrac{\partial^2 d}{\partial x^2} + \chi_d r_2 \end{cases} \qquad (31)$$

where x is a dimensionless axis (normalized by d_b), normal to the interface and oriented towards the bulk of the liquid phase, and t is the dimensionless time (normalized by d_b/G).

At $x=0$ (corresponding to the interface), a concentration condition is imposed for the a specie and an isolation condition is imposed for the other species:

$$a = 1 \ , \ \frac{\beta_b}{Pe}\frac{\partial b}{\partial x} = 0 \ , \ \frac{\beta_c}{Pe}\frac{\partial c}{\partial x} = 0 \ , \ \frac{\beta_d}{Pe}\frac{\partial d}{\partial x} = 0 \quad (32)$$

For $x \to \infty$ (bulk of the liquid), a no flux condition is imposed for each species:

$$\frac{1}{Pe}\frac{\partial a}{\partial x} = 0 \ , \ \frac{\beta_b}{Pe}\frac{\partial b}{\partial x} = 0 \ , \qquad (33)$$

$$\frac{\beta_c}{Pe}\frac{\partial c}{\partial x} = 0 \ , \ \frac{\beta_d}{Pe}\frac{\partial d}{\partial x} = 0$$

The initial condition is:

$$a = \alpha \ , \ b = 1 \ , \ c = 1 \ , \ d = 1 \qquad (34)$$

The Sherwood number is calculated by the time integration from $t=0$ to $t=1$ of the instantaneous dimensionless a flux at $x=0$, as follows:

$$Sh_{Higbie} = -\frac{1}{1-\alpha}\int_0^1 \frac{\partial a}{\partial x}dt \qquad (35)$$

As the Higbie approach is based on the assumption that the liquid in contact with the bubble slips on the interface, the simulation results for the clean bubble case are then compared to the numerical resolutions of these equations, which has been realized in a previous work [10].

The comparison is presented in Figure 8. An excellent agreement between these two approaches is observed. Concerning the enhancement factor, the Higbie approach provides an excellent estimation for $Ha_1 \leq 1$. For $Ha_1 > 1$, the Higbie approach tends to slightly underestimate the effect of chemical reactions.

(a)

(b)
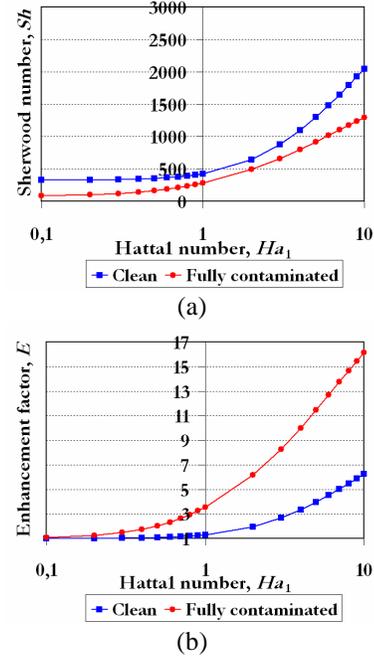
Figure 7. Sherwood number (a) and enhancement factor (b) versus Hatta1 number for clean and fully contaminated bubbles.

(a)

(b)
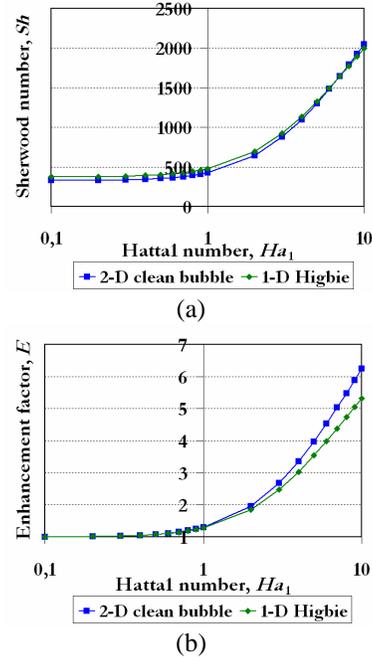
Figure 8. Sherwood number (a) and enhancement factor (b) versus Hatta1 number for 2-D clean bubble approach and 1-D Higbie approach.

5. Conclusions and Futures Plans

In this paper, COMSOL Multiphysics is used successfully to model a 2-D spherical bubble rising in a liquid. Two cases are investigated: a clean bubble and a fully contaminated bubble behaving as a solid sphere.

This model is developed to estimate the CO_2 transfer rate from bubble to the brine in a BIR bubble column. In this system, chemical reactions are coupled with the mass transport.

The model is first validated in the case without reactions by comparing successfully the computed drag coefficient, separation angle (for the fully contaminated bubble only) and Sherwood number (dimensionless transfer rate) with correlations from the literature.

The model is used to estimate the Sherwood number and the enhancement factor as a function of the Ha_1 number (dimensionless reaction rate of the reaction 1) for both clean and fully contaminated bubble.

The results show the increase of the mass transfer rate with increasing chemical reaction rate. The enhancement effect of the chemical reaction rate is more important in the fully contaminated bubble case than in the clean bubble case.

More, the simulations results related to the 2-D clean bubble are compared with a 1-D Higbie model results computed in a previous work. An excellent agreement is observed until $Ha_1=1$. For higher value, the 1-D model tends to slightly underestimate the enhancement effect of the reactions.

This result tends to validate the approach 1-D modeling, commonly used in chemical engineering to estimate the interfacial mass transfer rate.

The future plan is to extent this model to a larger bubble case, with diameter from 2 to 6 mm that have an ellipsoidal shape and a Reynolds number from $Re=400$ to $Re=1200$. The shape of the bubbles will be provided from data of an experimental device which is currently on operation.

6. References

1. R. Clift, J.R. Grace and M.E. Weber, *Bubbles, drops and particles*. Dover Publications, Mineola (1978)

2. B. Haut, Contribution à l'étude des colonnes à bulles mettant en œuvre une réaction de précipitation, PHD thesis, ULB (2004)

3. R.D. Vas Bhat, J.A.M. Kuipers and G.F. Versteeg, Mass transfer with complex chemical reactions in gas–liquid systems: two-step reversible reactions with unit stoichiometric and kinetic orders, Chemical Engineering Journal, **10**, 127-152 (2000)

4. A.H.G. Cents, D.W.F. Brilman and G.F. Versteeg, CO_2 absorption in carbonate / bicarbonate solutions: The Danckwerts-criterion revisited, Chemical Engineering Science, **60**, 5830-5835 (2005)

5. A. Dani, A. Cockx and P. Guiraud, Direct Numerical Simulation of Mass Transfer from Spherical Bubbles: the Effect of Interface Contamination at Low Reynolds Numbers, *International Journal of Chemical Reactor Engineering*, **4**, A2, (2006)

6. R.B. Bird, W.E. Stewart and E.N. Lightfoot, *Transport Phenomena*, John Wiley&Sons, New York (2002)

7. V.G. Levich, *Physicochemical hydrodynamics*, Prentice-Hall, USA (1962)

8. P. Trambouze and J.-P. Euzen, *Chemical reactors: from design to operation*, TECHNIP, France (2004)

9 J.M. Coulson and J.F. Richardson, *Chemical Engineering: fluid flow, heat transfer and mass transfer, vol.1*, Butterworth Heinemann (1999)

10. C. Wylock, P. Colinet, T. Cartage and B. Haut, Coupling between mass transfer and chemical reactions during the CO_2 absorption in a $NaHCO_3$-Na_2CO_3 brine: experimental and theoretical study, *International Journal of Chemical Reactor Engineering*, vol. 6/A4 (2008)

7. Acknowledgements